REPORT DOCUMENTATION PAGE

Form Approved
OMB No. 0704-0188

1. AGENCY USE ONLY (Leave blank)	2. REPORT DATE	3. REPORT TYPE AND DATES COVERED
	Jan 10-13, 1983	

4. TITLE AND SUBTITLE
UNSTEADY FLOW SEPARATION AND ATTACHMENT INDUCED BY PITCHING AIRFOILS

5. FUNDING NUMBERS
(2)

6. AUTHOR(S)
M.C. Robinson
M.W. Luttges

7. PERFORMING ORGANIZATION NAME(S) AND ADDRESS(ES)
University of Colorado
Boulder, CO

8. PERFORMING ORGANIZATION REPORT NUMBER
AFOSR
81-0057

9. SPONSORING/MONITORING AGENCY NAME(S) AND ADDRESS(ES)
AFOSR
BLDG 410
BAFB DC 20332-6448

AFOSR-TR 90-0028

10. SPONSORING/MONITORING AGENCY REPORT NUMBER

11. SUPPLEMENTARY NOTES

12a. DISTRIBUTION/AVAILABILITY STATEMENT
Unlimited

12b. DISTRIBUTION CODE

13. ABSTRACT (Maximum 200 words)

14. SUBJECT TERMS

15. NUMBER OF PAGES
14

16. PRICE CODE

17. SECURITY CLASSIFICATION OF REPORT	18. SECURITY CLASSIFICATION OF THIS PAGE	19. SECURITY CLASSIFICATION OF ABSTRACT	20. LIMITATION OF ABSTRACT
unclassified	unclassified		

[illegible] OF INDUCED, SEPARATED VORTICES GENERATED BY [illegible] AIRFOILS

Michael C. Robinson*
and
Marvin W. Luttges**
University of Colorado
Boulder, Colorado 80309

Abstract

The dynamics of induced, separated vortices generated from sinusoidal airfoil oscillations were examined across a range of unsteady flow parameters. Leading edge vortical initiation, development, and interaction with trailing edge vorticity were summarized via stroboscopic flow visualization and hotwire anemometry. Results indicate the sensitivity of vortical development at both leading and trailing edges to reduced frequency parameter and magnitude of oscillation angle. Certain optimal parametric conditions resulted in dramatic interactions of leading and trailing edge vorticity. At diminished oscillation angles, separated flow attachment was evident in the absence of the large induced vortical structures characteristic of large oscillation amplitudes.

Nomenclature

c	airfoil chord
K	reduced frequency, $\omega c/2V_\infty$
Re	Reynolds number, $V_\infty c/\nu$
T	time
V_∞	freestream velocity
α	angle of incidence, $\alpha = \alpha_m + \alpha_\omega \cos(\omega T)$
α_m	mean angle of incidence
α_ω	oscillation amplitude
ν	kinematic viscosity
ω	rotational frequency, rad/sec

Introduction

Unsteady aerodynamic effects generated by dynamically oscillating airfoils represent a major area of research in modern fluid mechanics.[1] When a lifting surface oscillates about a mean angle of attack in excess of its static stall angle, large, unsteady aerodynamic forces are produced. The unsteady lift, drag, and moment coefficients can greatly exceed the expected static counterparts. These forces are directly related to the stall caused by transient separation of the flow from an airfoil dynamically oscillating in pitch. Stall of this nature is classified as dynamic stall. The occurrence and severity of dynamic stall is directly related to the type of airfoil, Reynolds number, oscillation rate, and oscillation amplitude. Inherent in dynamic stall is the formation of leading edge vortices; these vortices can produce a surge in the lift force as well as unsteady moments on the airfoil.[2] It is believed that repetitive generation of dynamic stall vortices might be exploited to delay stall or energize the flow field to greatly increase the operating characteristics of an airfoil past its static stall angle (cf. Ref. 3).

Another energized structure generated from airfoil oscillation is the trailing edge vortex. The circulation of the trailing edge vortex is opposite in direction to the vorticity generated at the leading edge, and appears to be linked to passage of the leading edge vortex. The overall contribution to the dynamic stall process from trailing edge vortical development has not been well defined.[4,5] Similarly, the effects of the leading edge-trailing edge vortical interaction are still being quantified, again stressing the need for all types of unsteady flow data.[6]

The exact mechanisms underlying the formation of dynamic stall vortices have been a topic of study for much of the 20th century.[1] The complexity of the unsteady forces has slowed the emergence of numerical prediction methods. Theoretical studies of unsteady airfoil phenomena revolve around attempts to relax assumptions postulated in steady thin airfoil theory, but significant progress has been elusive. Experimental studies are similarly complicated, involving various airfoil types and modifications designed to enhance vorticity production over a broad range of both static and dynamic flow parameters.[7,8] The general thrust of experimental research has been to reduce the undesirable effects associated with dynamic stall. Normally, tests were done with airfoils driven through large, slow oscillations in angle of attack. In contrast, small amplitude and relatively high speed oscillations in angle of attack may be more consistent with practical applications and technical feasibility.

The unsteady effects of dynamic stall are characterized by turbulent separated flow and vortical structures. Two prevalent theories have been formulated regarding the occurrence of vortices during dynamic stall. One suggests that the transient bursting of laminar separation bubbles leads to vortices.[9] The laminar separation bubble is formed during transitions from a laminar to an attached turbulent flow. When the separation point progresses to the base of the bubble, the bubble bursts and induces a vortical structure. The second approach envisions an abrupt turbulent separation over the front portion of the airfoil; this turbulent separation is thought to be responsible for the production of dynamic stall vortices.[7] The boundary layer may remain totally laminar prior to separation, and this, by definition, precludes the formation of a laminar separation bubble. Both mechanisms of vorticity production are associated with the dynamic separation of the flow, although some critical parameters may vary in relation to the dominance of one or the other mechanism.

Vortical structures appear to be important correlates of the unsteady stalling of an airfoil. There seem to be two favored methods by which these important structures may be experimentally enhanced: (1) by continued increments of airfoil angle past the turbulent separation point,[7] and (2) by abruptly changing the pitch direction of the airfoil shortly after the turbulent separation of the flow has occurred.[6]

In the following studies, abrupt changes in pitch direction of the airfoil were achieved using small oscillation angles ($2°$-$5°$) at high speed (11 Hz)

*Graduate Research Assistant, Department of Aerospace Engineering Sciences. Member AIAA.

**Professor, Department of Aerospace Engineering Sciences.

pitch oscillations to elicit repetitive vortical structure. Extensive flow visualization was used in conjunction with hotwire anemometry to characterize the initiation, development, and migration of the vortex through the oscillatory cycle. The evaluation of independent static and dynamic variable combinations focused upon those that might maximize exploitable aerodynamic phenomena from vortex development. Of principal interest were the utility of the reduced frequency parameter in characterizing flow disturbance from reduced oscillation angles, and the formation and development of trailing edge vortical structure.

Methods

Experiments were conducted on NACA 0012 and NACA 0015 airfoils in the low-turbulence 2' × 2' wind tunnel at the University of Colorado. Flow field measurements were obtained via flow visualization in conjunction with hotwire anemometry.

A solid aluminum NACA 0012 with 10-inch chord and a hollow-core NACA 0015 with 6-inch chord, both with a 2-foot (infinite) span, were used for the experiment. The airfoils were driven through pitching motions with a 1/3-H.P. D.C. motor using a 6-to-1 gear reduction connected to a variable displacement scotch yoke. Sinusoidal oscillation rate could be held constant while the magnitude of angle pitch was changed by adjusting the radial bearing on the flywheel of the D.C. motor. The angle around which the oscillatory cycle occurred was determined by initial positioning of the wing in the drive yoke. A rotating potentiometer on the flywheel was used to determine the angular velocity and specific attitude of the airfoil during any portion of the rotation cycle.

Flow visualization was obtained using a smoke rake constructed of a NACA 0015 airfoil with 1/8-inch diameter tubes inserted in the trailing edge. The smoke rake was located in the settling chamber of the 2' × 2' wind tunnel in order to minimize disturbances to the test section. The rake could be moved vertically to optimize the position of the smoke lines. Dense smoke was generated from heated Rosco fog juice stored in a 55-gallon drum and delivered to the rake at modest pressure. The pressure and ensuing flow rates were adjusted to prevent smoke from being emitted as a turbulent jet.

Synchronization of data acquisition with the airfoil angle during an oscillation was accomplished using the rotating potentiometer which produced a 0 to 5 volt ramp output corresponding with the 0 to 2π oscillation of the airfoil attitude. Voltage discrimination levels from 0 to 5 volts could be preset on the electronic trigger. When the selected voltage was reached during an oscillation, a 300-μsecond pulse was generated to trigger both the strobe for flow visualization and PDP 11/23 microprocessor for velocity measurements. In this manner, all angle-dependent data collection could be synchronized with the proper phase angle of the airfoil. All angle-dependent synchronization signals were checked regularly by stroboscopic examination of airfoil position relative to a fixed micrometer scale.

Single and multiple phase-locked stroboscopic (7 μsecond duration, point-source flashes) pictures were taken of the flow field, using a 35 mm SLR camera with ASA 400 film. The still photographs generated exact details of the vortical flow structure, whereas the phase-locked multiple-exposure photographs highlighted the repetitiveness of flow field disturbances.

Velocity measurements were made using a conventional constant temperature 2-needle hotwire probe, constructed of 0.0001-inch Wollaston wire. Using various linearizing circuits referenced elsewhere,[10] a 0 to 5 volt output was generated proportionally to the mean flow. The hotwire probe was mounted on an orthogonally driven traversing mechanism in the airfoil test section.

Hotwire data acquisition and subsequent reduction were accomplished with a PDP 11/23 microprocessor. Upon receipt of a 300-μsecond pulse from the phase-lock trigger, the analog hotwire signal was digitized and stored at a sampling frequency of 1000 Hz. At each pulse, data were collected over two complete oscillation cycles representing one data run. Ten such successive data runs were averaged to reduce the signal noise and accent the periodic disturbances generated during the oscillatory cycle.

Results

Stall angles for the NACA 0012 airfoil were determined photographically to be approximately $\alpha = 10.9$ at a Reynolds number of 100,000. In static testing at these angles of attack, the streamlines clearly lifted from the airfoil surface as the flow neared the trailing edge. Turbulent flow was observed in the area from which the streamlines had separated. In most instances, the flow was not attached over the last 2 inches of the 10-inch chord airfoil. The NACA 0015 airfoil exhibited separated flow at just slightly higher ($\approx 0.5°$) angles of attack. These flow patterns for both airfoils were used for comparisons with the various dynamic conditions reported below.

Depending on test parameters, a number of reproducible flow perturbations were characteristic of the airfoils during oscillation. Many of these perturbations have been described previously for different test parameters (cf. Ref. 11). The most prominent flow disturbances were the formation of a leading edge vortex, the movement of the vortex along the airfoil surface, changes in vortex structure, interactions between the vortex and the airfoil, interactions between the vortex and the free-stream flow, interaction of the vortex with the trailing edge of the airfoil, formation of a trailing edge vortex, and interactions between leading and trailing edge vortices, both at the trailing edge and in the airfoil wake. Most of these disturbances were stable enough during each portion of the oscillatory cycle to permit repeated stroboscopic ($\approx$ 7 μseconds) illumination for multiple ($\geq$ 20)-exposure photographs.

When a leading edge vortex is generated, the growth characteristics of the vortex during the remaining portions of the oscillatory cycle and across time appear quite constant. A small vortex is identifiable near the leading edge as the airfoil pitches toward the maximum angle of attack (Fig. 1, 0 % cycle). The vortex increases in physical magnitude as it moves across the airfoil surface toward the trailing edge (Fig. 1, 25 % cycle). In the presence of large vortices, flow separation occurs over the entire airfoil chord as the vortex interacts with the trailing edge and sheds into the wake. Shedding occurs as the airfoil approaches the bottom of the downstroke (minimum angle). Flow reattaches

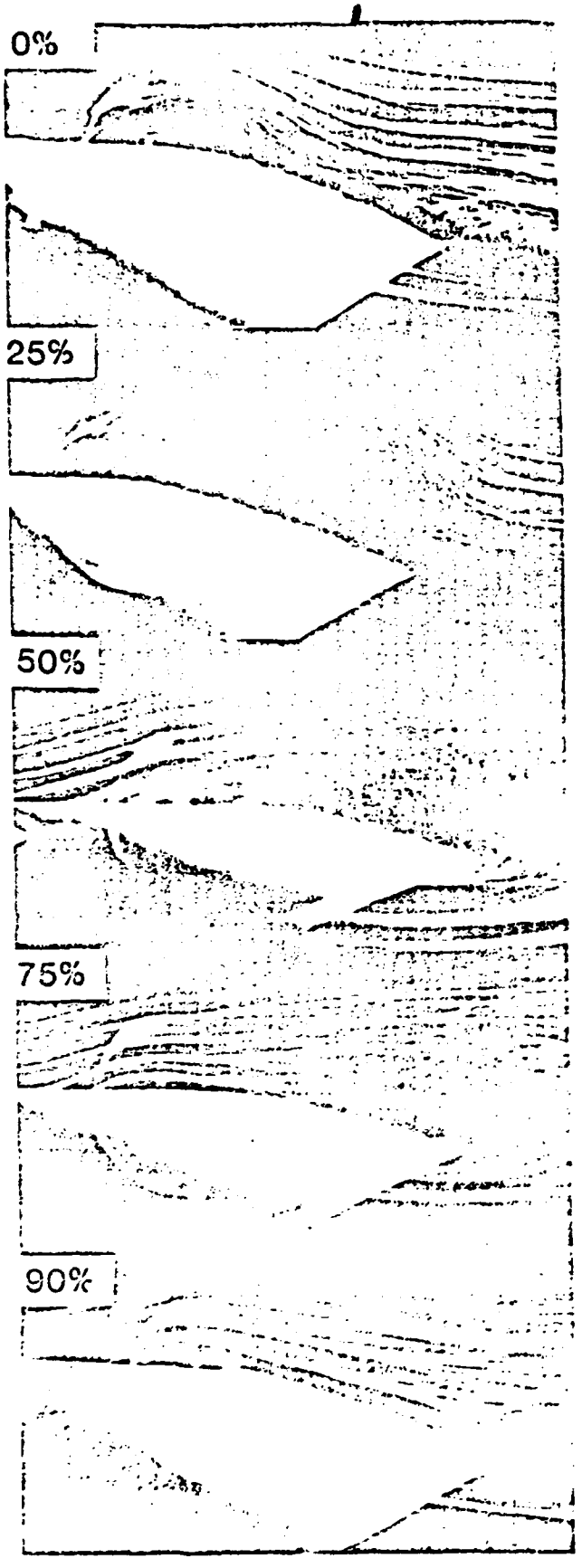

Fig. 1. Vortical development on airfoil surface at increasing periods in the airfoil cycle.
Re = 100,000; K = 0.5; α = 12.9° ±5°.

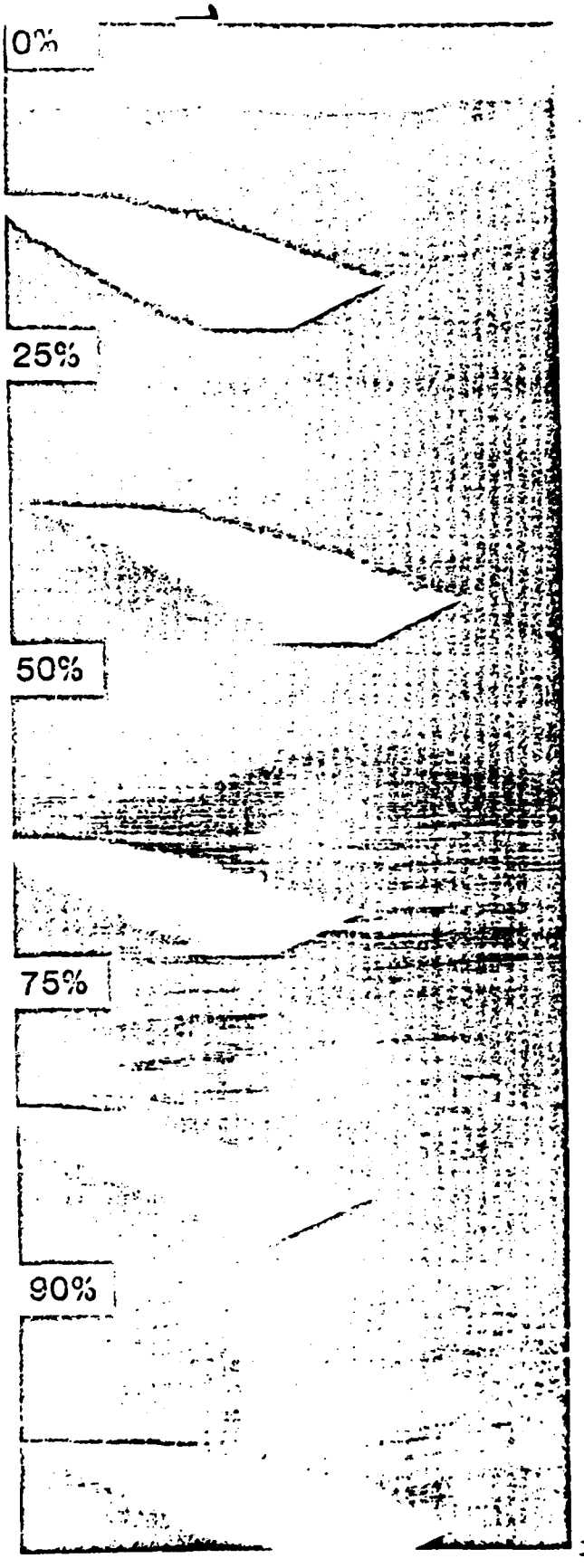

Fig. 2. Nonsynchronous vortical development at reduced oscillation angle.
Re = 60,000; K = 0.25; α = 12.9° ±1°.

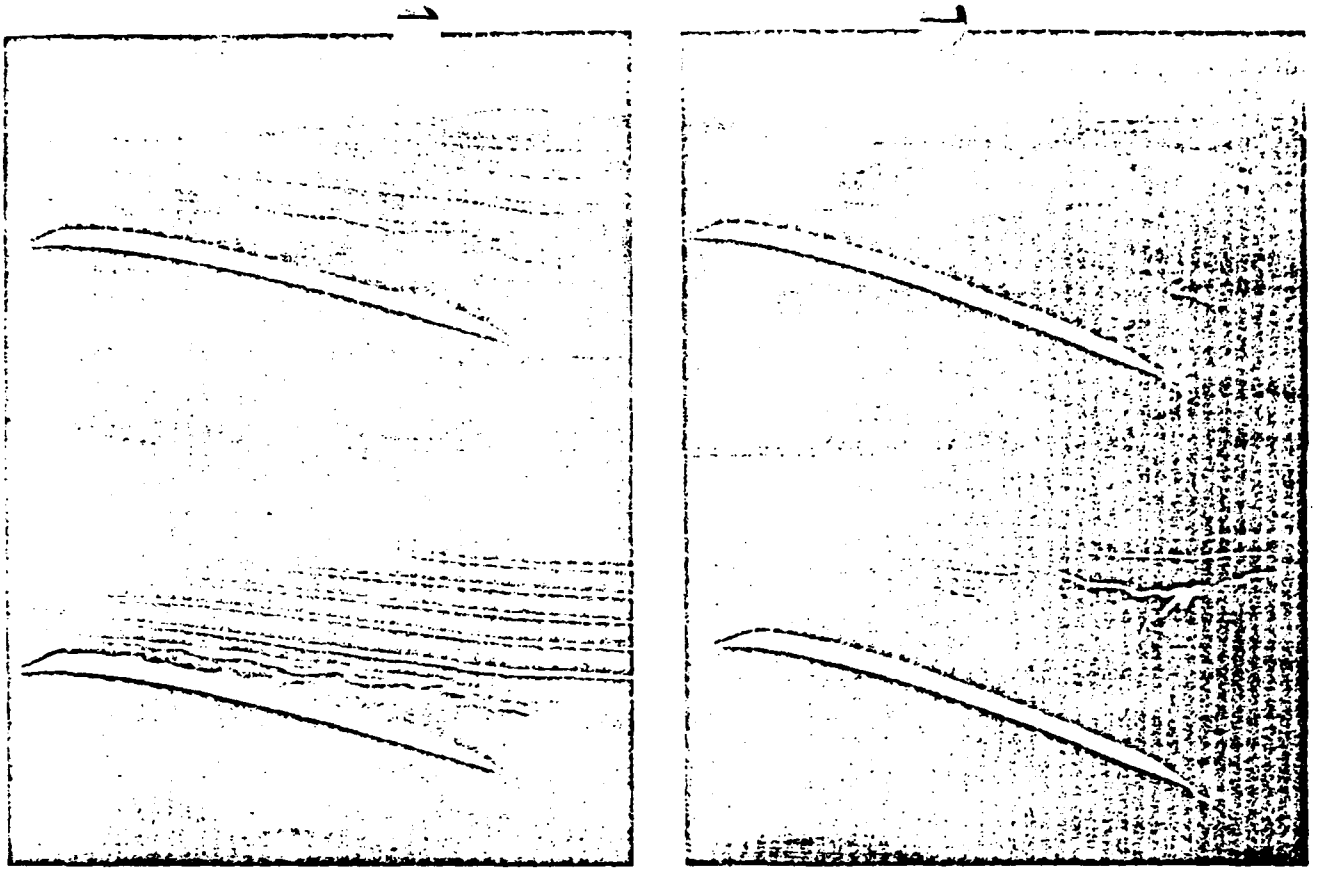

Fig. 3. Flow reattachment with increasing reduced frequencies. Re = 100,000; $\alpha = 13.9° \pm 0.5°$. Upper left: 25% cycle; K = 0.25. Lower left: 25% cycle; K = 1.25. Upper right: 75% cycle; K = 0.75. Lower right: 75% cycle; K = 1.25.

Fig. 4. Leading and trailing edge vortical development with instantaneous (≥ 7 μsec) single-exposure photographs. Re = 100,000; K = 0.5; $\alpha = 13.9° \pm 0.5°$. Left: leading edge. Right: trailing edge.

(Fig. 1, 75% cycle) as the pitch direction changes to the upstroke of the leading edge. These cyclic flow disturbances are repeated as the airfoil again nears the maximum angle of attack. Multiple-exposure photographs permit a clear distinction to be made between the steady, reproducible, synchronous flow effects linked to airfoil oscillation and the truly turbulent effects linked to more conventional elements of separation and stall.

Under oscillating conditions where a dynamic stall vortex is not apparent (Fig. 2, 0-75%), temporally repeatable flow field disturbances are more limited. Separation appears to be prevalent over the airfoil chord throughout the oscillation cycle.

Multiple-exposure photographs, however, tend to be misleading in determining whether or not weak vortical structures are present. In these instances of repeated exposures, it was difficult to distinguish between turbulence and weak but ordered disturbances, which tend to return flow to the airfoil

surface. Unless strong forces are acting to reattach flow at specific points in the oscillatory cycle or at specific points along the airfoil, the flow line disturbances may appear to have little direction.

Helin[12] recently showed that small oscillation angles can effectively reattach separated flow if they are used in conjunction with high oscillation rates (Fig. 3). Quantification of approximately 300 photographs revealed several conditions under which flow attachment at or before the trailing edge could be attained. Leading edge vortical development also was observed. Single, instantaneous (< 1 msec) visualizations of the flow revealed specific structures characteristic of flow perturbations caused by small oscillation angles and large oscillation rates (Fig. 4). Since the shedding of the weak vorticity was not tied precisely to the oscillatory frequency, the flow field appeared characteristically "blurred," suggesting turbulent separation (Fig. 2). More accurately, large oscillation rates at reduced oscillation angles induced flow attachments that were poorly synchronized both spatially and temporally with the oscillation parameters. Similar vortical development, induced by leading edge separation, was observed at most static stall angles. During oscillation, however, a characteristic bending of the flow toward the airfoil surface occurred before the flow reached the trailing edge of the airfoil. This flow reattachment inevitably occurred during the downstroke portions of the oscillatory cycle. The higher oscillation rates (higher values of K) were associated with flow reattachments appearing well before the trailing edge was reached. Thus, the flow disturbances summarized below seem to belong to a continuum of dynamic effects that originate with small angle rapid oscillations, which induce relatively modest flow disturbances, and include larger angle rapid oscillations, which elicit relatively strong flow disturbances.

In order to determine the effects of the flow variables on vortical development, a photographic parametric study was conducted across a range of independent variables (Table 1). As expected, the only condition that did not generate clearly discernible vortical structures in multiple-exposure flow visualization photographs was the oscillation angle ±1° around modest fixed values of α. As indicated above, any elicited vortical structures were undoubtedly poorly synchronized with the oscillatory cycle. Even oscillation angles of ±3° generated only modestly synchronized vortex structures in multiple-exposure photographs obtained at Reynolds numbers of 100,000 to 140,000. At a Reynolds number of 60,000, any vortices generated by ±3° oscillations were embedded in other, more random, flow disturbances. In these flow visualization studies, the largest and most well-synchronized vortices occurred at increased values of the reduced frequency parameter, at higher angles of attack, and at higher oscillation angles. Changes in Reynolds number did not have major effects on vorticity across the values tested in the present study.

The creation and fate of the highly synchronized, strong vorticity were carefully characterized in order to determine which flow disturbances were attributable to such strong vorticity. From the photographs (12/cycle), the movement of the vortex center was plotted as it migrated across the airfoil surface from leading to trailing edge (Fig. 5). The slope of the line representing vortex position on the airfoil for increasing times during a single oscillation cycle represents the apparent mean velocity of the vortex center over the airfoil. On the average, the velocity of vortex movement from the leading to the trailing edge of the airfoil was 35-45% V_∞. Whereas straight line segments on these plots indicate a uniform velocity of vortex movement from leading to trailing edge, curvature and/or discontinuity corresponds to a delay or hesitation in the movement of the vortex center. The more clearly defined curvatures in these plots indicate maximum delays, and correspond to the presence of the largest vortical structures observed. The reduced frequency parameter (K) was very useful in predicting the relative position of the vortical center over the airfoil surface during the oscillation cycle, for a variety of Reynolds numbers and oscillation angles. However, the delays in vortex movement over the airfoil surface could not be predicted from the values of K employed in these tests.

Table 1

Independent Variables for Photographic Study

Reynolds Number	Reduced Frequency	Mean Angle	Oscillation Angle
60,000	0.25, 0.5, 0.75	12.9°	1°, 3°, 5°
100,000	0.25, 0.5	12.9°	1°, 3°, 5°
140,000	0.25	12.9°	1°, 3°, 5°

It should be noted that this parametric study was performed without endplates on the oscillating airfoil. As also found by Carr et al.,[11] the tunnel wall effects on vortical generation mechanisms were negligible at both the elevated values of K and the large fixed values of α examined in the present study. A series of photographs taken both with and without endplates at a Reynolds number of 60,000, K = 0.25, and α = 15° ±5° showed no discernible change in the overall flow disturbances visualized at mid-span of the airfoil. The endplates were abandoned for the remaining tests since they placed a great deal of stress on the oscillation drive mechanism, and they severely limited the oscillation rates that could be employed in subsequent tests.

In order to characterize the magnitude of the velocity disturbances generated by the leading edge vortex, linearized hotwire measurements were made over three chord locations at various positions above the airfoil surface (Table 2). The probe location was held fixed relative to the wind tunnel while the airfoil was oscillated. For each test, data were collected for oscillation-phase triggered, single velocity profiles across two successive complete oscillation cycles. Ten such individual runs were trigger-synchronized in order to match corresponding initial angles of attack, and to permit numerical

Table 2

Independent Variables for Hotwire Study

Reynolds Number	Reduced Frequency	Mean Angle	Oscillation Angle
60,000	0.25, 0.5	0°, 15°	1°, 5°
100,000	0.25, 0.5	15°	1°, 5°
140,000	0.25	0°, 15°	1°, 5°

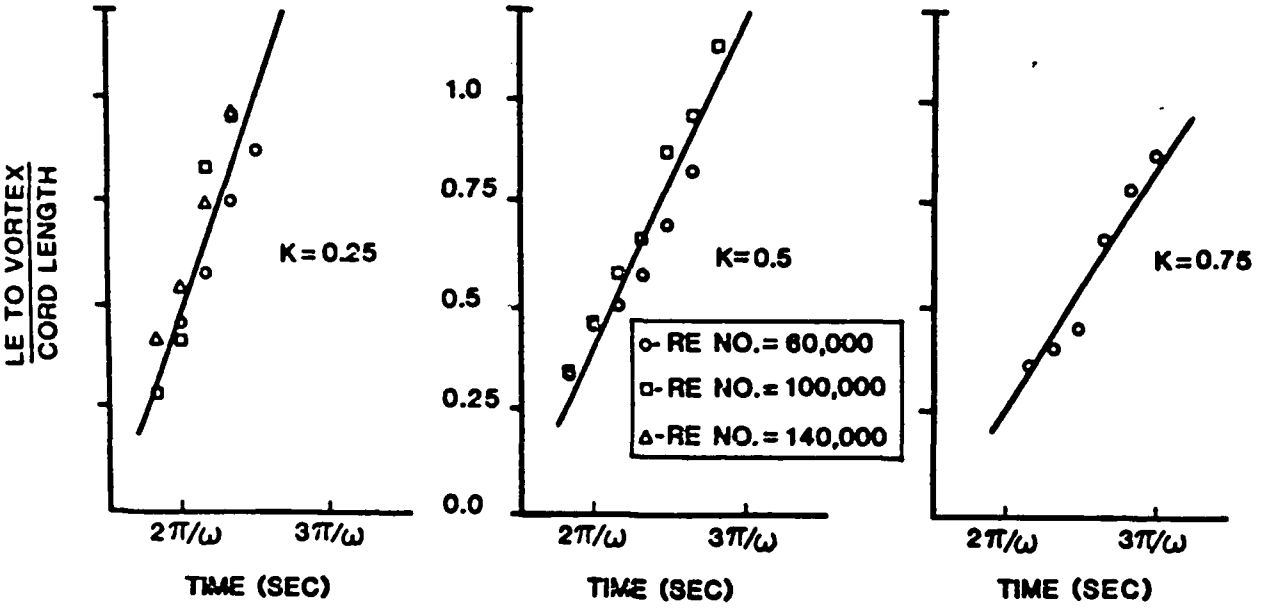

Fig. 5. Vortex center location on airfoil surface during the oscillatory cycle.

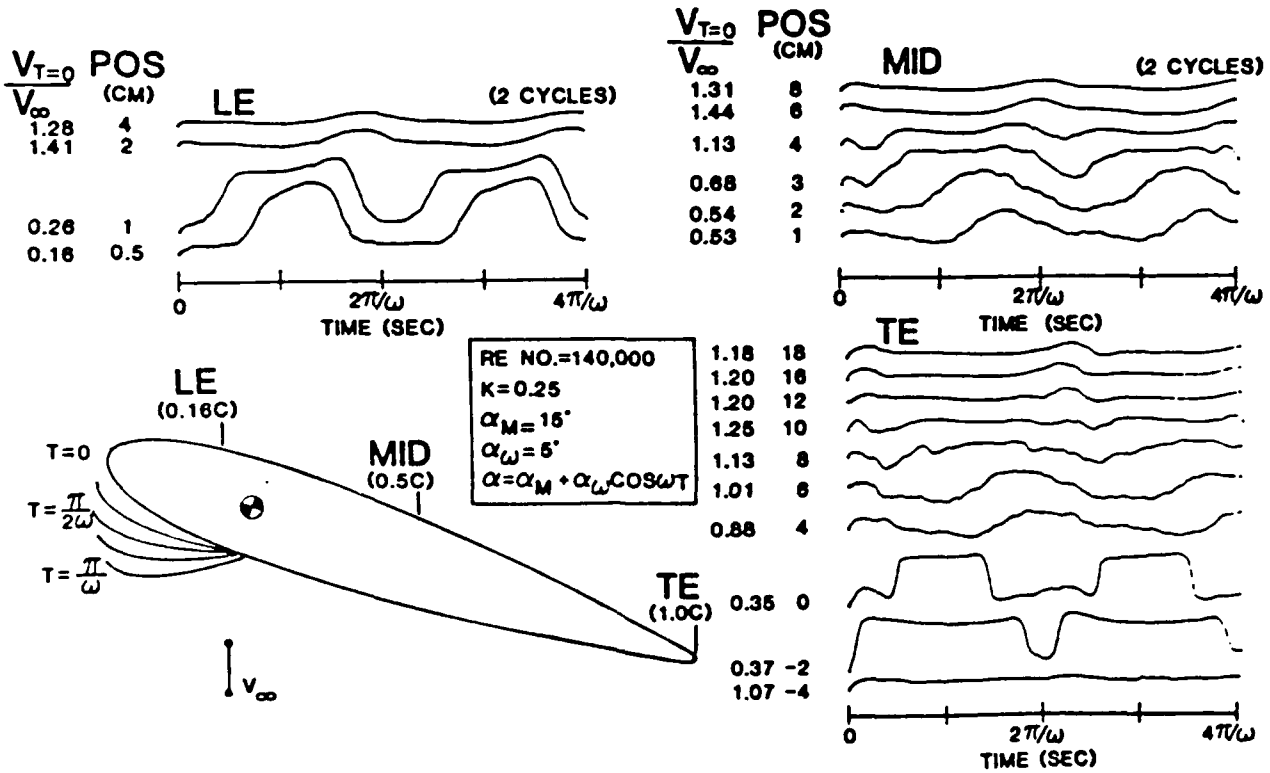

Fig. 6. Velocity measurements at selected points during synchronous vortical development.

averaging. The synchronous triggering also allowed correlations of the hotwire measurements with flow visualization. Figure 6 is a typical example of the averaged hotwire measurements obtained for a two-cycle period. The velocity magnitudes correspond to the instantaneous velocity components at T = 0 (maximum angle of attack). Velocities at subsequent times in the oscillatory period were obtained from the hotwire signal traces. Position refers to the distance of the hotwire probe from the airfoil surface (in cm) when the angle of attack was at the mean oscillation angle.

Figure 6 is illustrative of the results obtained for a set of experimental conditions that generate strong, synchronous vorticity in the flow. At the leading edge (T = 0, 0.5 cm) the probe was closest to the airfoil for the bottom two traces.

Throughout the oscillatory cycle, only minimal velocities were noted at these positions in the flow field. As the airfoil moved through the oscillation cycle, a velocity maximum occurred ($T = \pi/\omega$) as the airfoil attained the minimum angle of attack. Since the probe was no longer shielded from the freestream by the leading edge of the airfoil, it appeared to record the unobstructed velocity maximum. The hotwire velocity profiles indicated a similar type of blockage effect when the probe was located at the airfoil trailing edge. At $T = 0$ (maximum angle) the trailing edge was beneath the hotwire probe, effectively shielding the probe from the freestream velocity. As the airfoil angle decreased, the velocity measurement grew to maximum coincident with the passing of the trailing edge to positions above the probe location.

At probe positions in excess of 8 cm above the trailing edge, 6 cm above mid-chord, and 2 cm above the leading edge, other periodic maxima occurred during the cycle. These maxima appear to reflect the velocity induced by the passage of the leading edge vortex across the airfoil surface. The larger the perturbation, the larger the magnitude of the shedding vortex. As the vortex size increased, the velocity fluctuations became more pronounced throughout the entire spatial grid of flow measurements around the airfoil.

The phase relations between the hotwire disturbance caused by the passing vortex in the far field and the maximum hotwire disturbances in the near field close to the airfoil surface at the trailing edge do not necessarily correspond to each other in a simple fashion. It will be shown subsequently that a vortical disturbance induced at the trailing edge and the leading edge vortex in the far field result in the strongest vortical development and interactions. Once vorticity is initiated, oscillation phase angles appear clearly secondary to these strong vortical interactions.

Another temporal effect of the shedding vortex can be seen in Fig. 6. A maximum velocity disturbance occurred at the leading edge at approximately the maximum angle of attack ($T = 0$). This maximum was seen both at later time periods and later portions of the oscillation cycle at the mid-chord and finally at the trailing edge. The delay in the velocity perturbation appearance at these sites was presumably an indication of the time required for the vortex to pass from the leading to the trailing edge of the airfoil.

Synchronous, spatially discrete disturbances were not generated at small mean angles for the Reynolds numbers and reduced frequencies tested (Fig. 7). Flow remained attached over the airfoil surface throughout the entire oscillation cycle. Velocity measurements at the trailing edge (Fig. 8, 0 cm, $\alpha = 0°$) show the response of the hotwire probe to the airfoil oscillation. Two separate velocity minima occurred in each cycle as the hotwire probe was aligned with the trailing edge. It was necessary to increase the mean angle until the critical stall angle was exceeded during an oscillation in order to generate strong leading edge vortices. At $\alpha = 0° \pm 5°$, two standing vortices developed, one each on the upper and lower surfaces of the trailing edge of the airfoil. Though relatively small in size (≈ 0.1 c in diameter), these disturbances remained over the complete oscillatory cycle of the airfoil with a circulation in the same direction as the leading edge vortex. Similar trailing edge vortical development was seen by these authors in studying the trailing edge generation of discrete audible tones.[13]

Small oscillation angles (Fig. 8) produced velocity fluctuations with little evidence for vorticity. The apparent "smooth" response of the hotwire signal, even under known flow separation conditions, was a result of averaging the hotwire signals over multiple oscillation cycles. In effect,

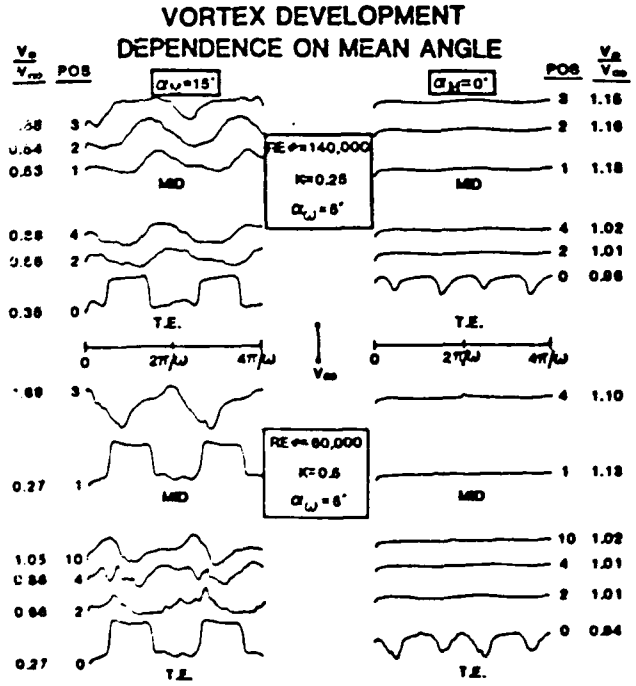

Fig. 7. Effects of mean angle on vortical development.

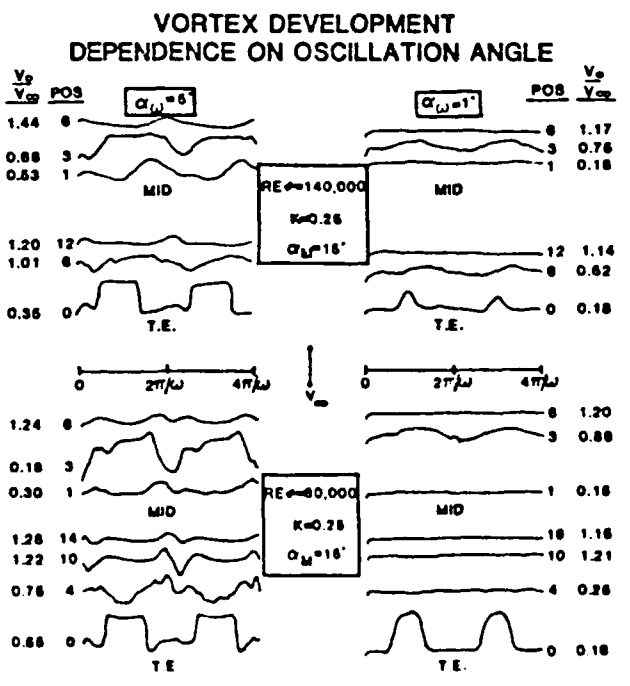

Fig. 8. Effects of small oscillation angle on vortical development.

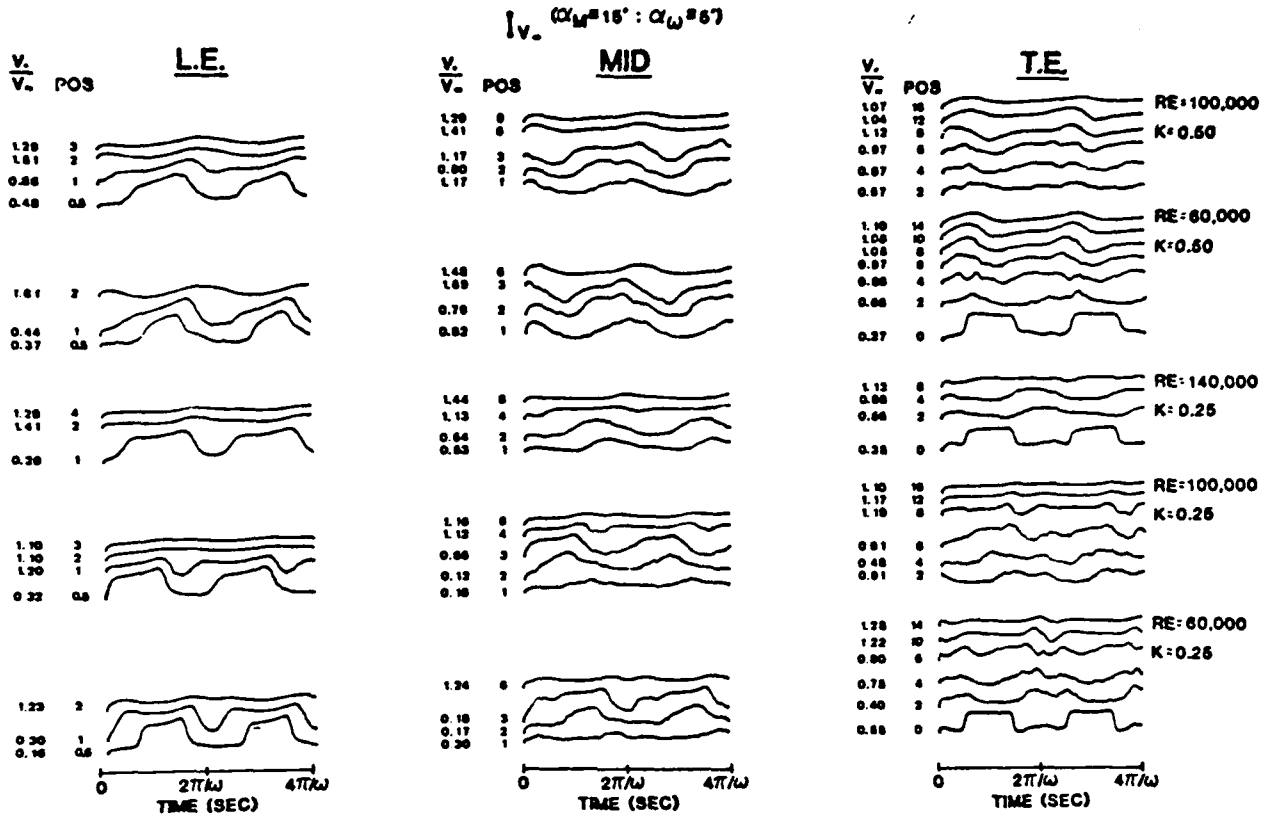

Fig. 9. Reynolds number and reduced frequency effects on vortical development.

the averaged velocity data indicated a lack of spatial and temporal synchrony between flow disturbances and airfoil motion. At certain positions above the trailing edge (Re = 140,000; $\alpha = 1°$; POS = 6 cm), velocity perturbations that were synchronized with the oscillating airfoil existed. Above and below those measurement points, however, the velocity disturbances were poorly correlated with airfoil oscillation cycle.

The effects of Reynolds number and the reduced frequency parameter on the passage of vorticity over the airfoil are given in Fig. 9. The strongest vortical disturbance (1.68 V/V_∞) occurred at a Reynolds number of 60,000 with a reduced frequency parameter of 0.5. Velocity measurements were normalized to freestream velocity in order to judge the relative contribution of each of the experimental parameters on vortical development and movement. With expanded plots of the same traces, it can be shown that the greatest time delays in the passing of vortices over the airfoil surface correlate positively with increasing strength. This was also shown to be true in the vortex location plots summarized in Fig. 5 for the quantified flow visualizations. It is important to note that each measure was obtained independently. In addition, the flow visualization relied predominantly on the use of the 10-inch chord NACA 0012 airfoil, while most of the hotwire anemometry (corroborated by visualization) relied on tests of the 6-inch chord NACA 0015 airfoil.

In general, velocities of the leading edge vortex increased with higher oscillatory frequencies (reduced frequencies). Increases in peak flow velocity of 5 to 8% were obtained when the reduced frequency was doubled from 0.25 to 0.5. When the reduced frequency was held constant, the velocity peak, corresponding to vortical passage, was inversely related to Reynolds number; increases in Reynolds number reduced the apparent velocities of the leading edge vortex. At reduced frequency of 0.25, the normalized velocity increased 16.8% as Reynolds number was reduced from 140,000 to 60,000. At K = 0.5, the normalized velocity increased 6.9% as Reynolds number was decreased from 100,000 to 60,000. These velocity increases were calculated from measurements over the trailing edge. When peak velocities were examined at mid-chord, changes in normalized velocity again showed an inverse relationship with Reynolds number. Increases in velocity magnitudes of only 2 to 3% were typical at mid-chord hotwire positions. Thus, small velocity decreases mid-chord were amplified into more striking decreases at the trailing edge. It was not clear if the vortical strength was actually reduced with increasing Reynolds number, or if the net velocity change at the trailing edge was simply a reflection of some other flow perturbation. Flow interactions produced as the leading edge vortex reached the trailing edge of the airfoil were the most likely causes of these vortical velocity differences.

Such a possibility prompted a detailed study

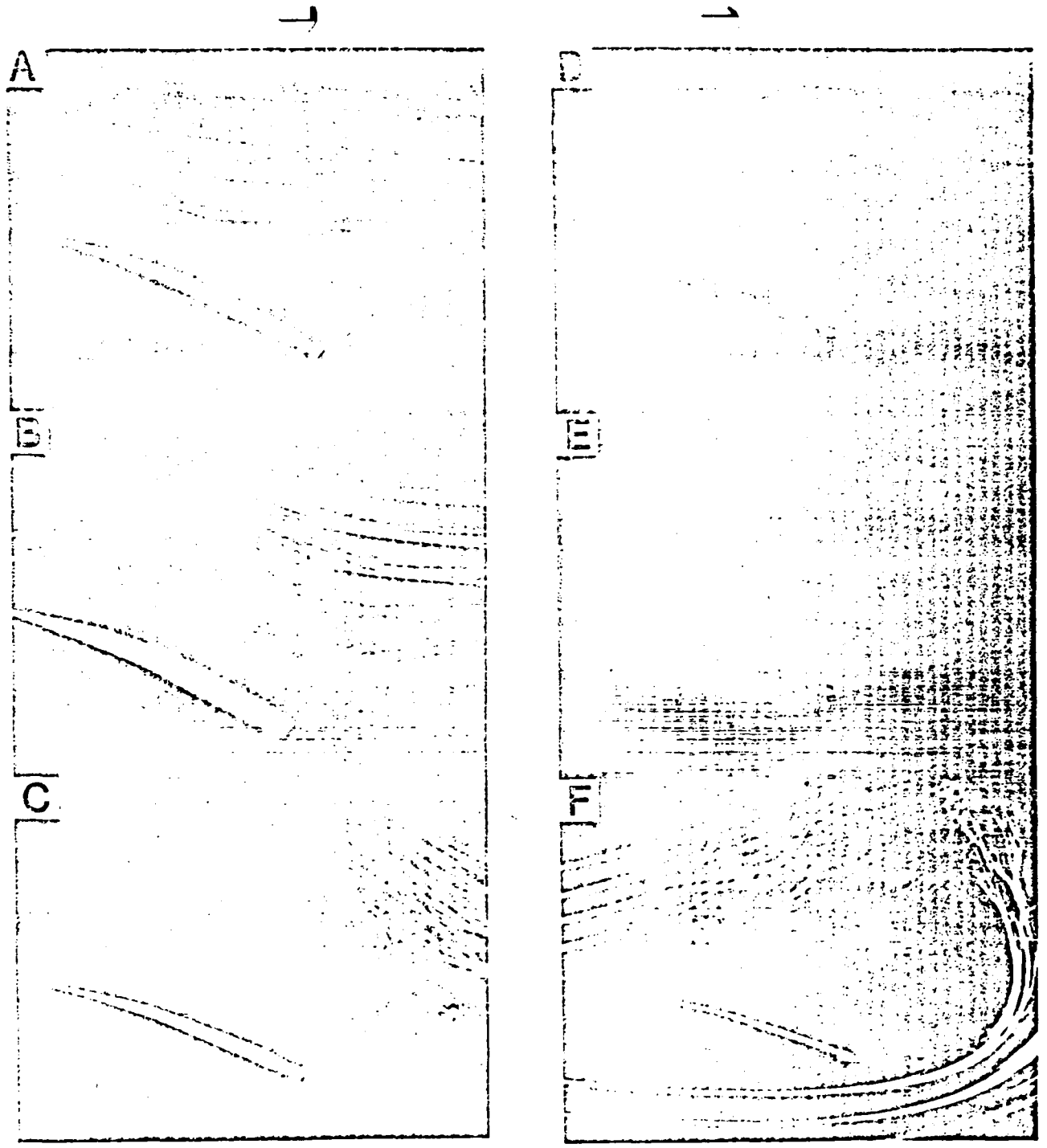

Fig. 10. The development of the leading edge vortex and the inducement of the trailing edge vortex.
(A) The airfoil attaining maximum pitch angle shows a vortex initiated at the leading edge.
(B) The downstream elements of the growing leading edge vortex appear mid-chord and bend streamlines toward the airfoil top surface.
(C) The growing vorticity shows downstream elements localized just ahead of the trailing edge.
(D) As the vortex passes the trailing edge, counter flow is induced from the bottom surface of the airfoil to the top surface. The surrounding streamlines are rapidly displaced from the airfoil surface.
(E) The trailing edge vortex exhibits rapid growth.
(F) The trailing edge vortex is shed into the wake immediately upstream of the remnants of the leading edge vortex.
Re = 60,000; K = 0.5; mean angle = 15° ±5°.
Approximately 20 exposures at each oscillatory phase angle.

of how the leading edge vortex interacted with all the elements of the surrounding flow. It was already amply clear that the leading edge vortex had one of the most dramatic influences on the overall flow field. Figure 10 depicts the sequence of flow interactions characteristic of a dynamic stall vortex when passing over the airfoil to the trailing edge and shedding into the wake. The series begins (Fig. 10A) as the vortex is generated near the leading edge and begins to move toward the trailing edge. At mid-chord (Fig. 10B), the rapidly increasing size of the vortex is evident. Corresponding temporally with the rapid growth, the vortex center slows its movement toward the trailing edge. The larger vortex covers much of the airfoil surface (Fig. 10C). As the vortex reaches the trailing edge, a flow reversal from flow around the trailing edge to the top surface of the airfoil occurs (Fig. 10D). The induced trailing edge vortex is generated with circulation opposite in direction to that of the leading edge vortex. Complete separation of the leading edge vortical flow from the airfoil surface occurs as the trailing edge vortex grows rapidly (Fig. 10E). The leading and trailing edge vortices combine into a tandem structure which sheds into the wake in unison. Within two chord lengths downstream of the airfoil, the size of the combined leading edge-trailing edge vortical structure exceeds the airfoil chord diameter by at least a factor of two; the flow lines exhibit dramatic vertical displacements suggestive of rapidly decelerating vorticity.

The induced trailing edge vortex possessed interesting small-scale characteristics. Rather than consisting of one small vortical structure which rapidly grew at the trailing edge, the vortex was composed of streamlines containing multiple smaller vortices. These small vortices ultimately coalesced into one large vortex. A similar flow phenomenon was recently observed by Freymuth[14] in his investigations of airfoils in linearly accelerating flows.

Whereas the leading edge vortex induced flow reattachment to the airfoil surface, the trailing edge vortex resulted in complete flow separation, which extended upstream to the leading edge. This total separation occurred as the trailing edge vortex reached maximum amplitude immediately prior to or coincident with shedding into the wake.

The striking interaction led to another photographic study. The initiation and interaction of the trailing edge vortex with the leading edge vortex were examined with variations in Reynolds number, reduced frequency, mean angle, and amplitude of oscillation. The parameters that affected the development of the trailing edge vortex paralleled results obtained for the leading edge vortex. Test conditions that generated the most temporally and spatially synchronous trailing edge vortices similarly produced the most temporally and spatially synchronous leading edge vortices.

The dependence of the trailing edge development on the mean angle of attack is illustrated in Fig. 11. The largest interactions between the leading and trailing edge vortices occur at greater ($\geq 15°$) mean angles of attack. At smaller angles ($\leq 5°$), the development of vortical instabilities is evident on both airfoil surfaces at the trailing edge. As noted earlier, similar vortical structures have been noted under nonoscillating conditions at small angles of attack and may be linked to boundary layer transition.

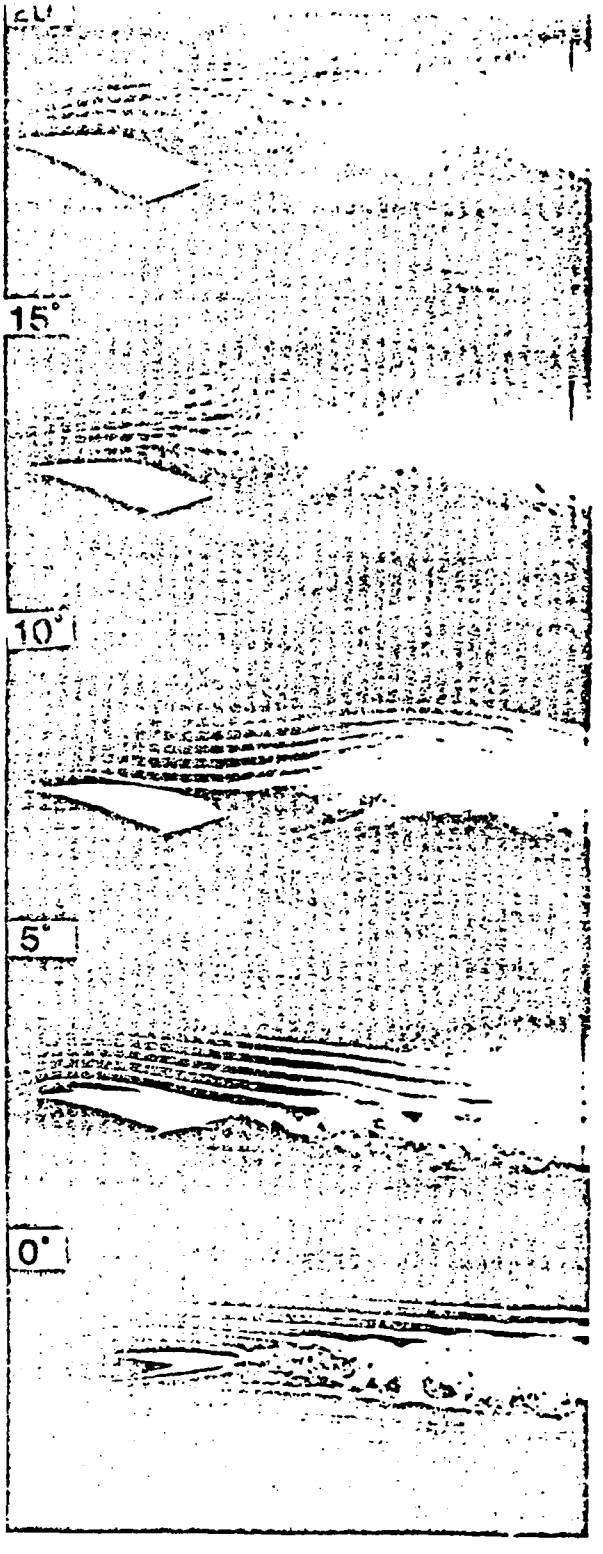

Fig. 11. Effects on the leading and trailing edge vortical interaction from variations in the mean angle of attack at Re = 60,000; K = 0.5; α_o = ±5°. Modest mean angles (20° and 15°) induce strong vortical interaction in the wake. Mean angles ≤10° elicit little temporally synchronous flow structure. At 0° and 5°, small temporally synchronous vortices shed into the wake from the airfoil trailing edge.

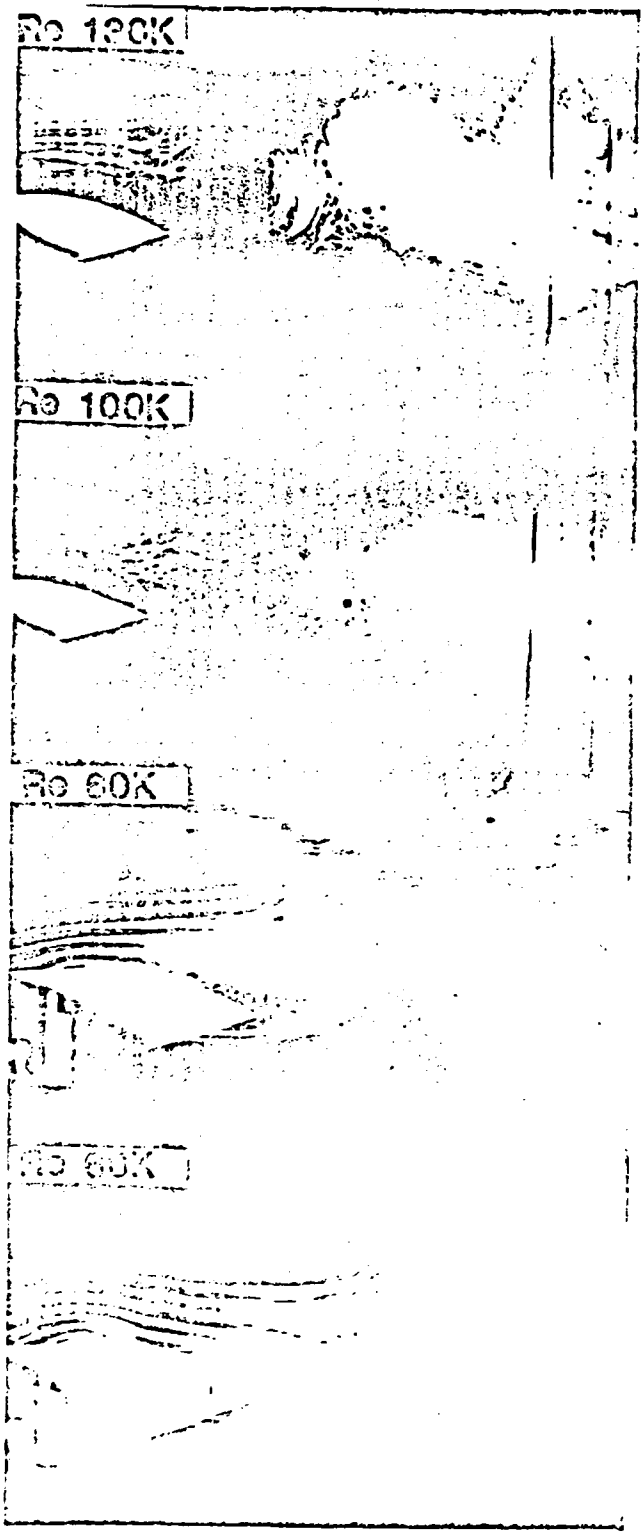

Fig. 12. Effects on the leading and trailing edge vortical interaction from variations in Reynolds number at α_m = 15°; α_ω = ±5°; K = 0.5. Strong interaction is evident at Re = 60,000; the bottom photograph was taken at a later point in the oscillatory cycle. Increases in Reynolds number (100,000 and 130,000) reduce the intensity of the interaction.

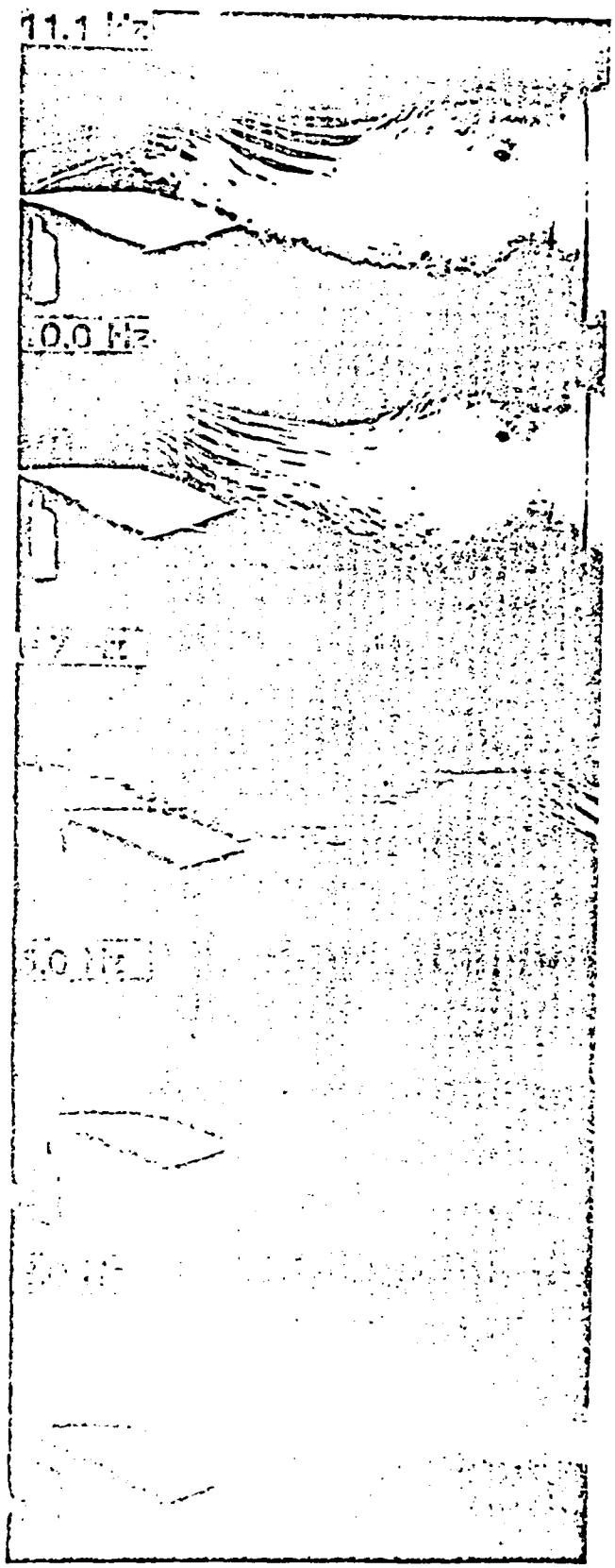

Fig. 13. Effects on the leading and trailing edge vortical interaction from variations in the oscillation frequency at Re = 60,000; α_m = 15°; α_ω = ±5°. From 11.1 to 5.0 Hz, temporally synchronous vortical interaction is evident. At 3.0 Hz, a reduction in the temporal dependence on airfoil oscillation occurs.

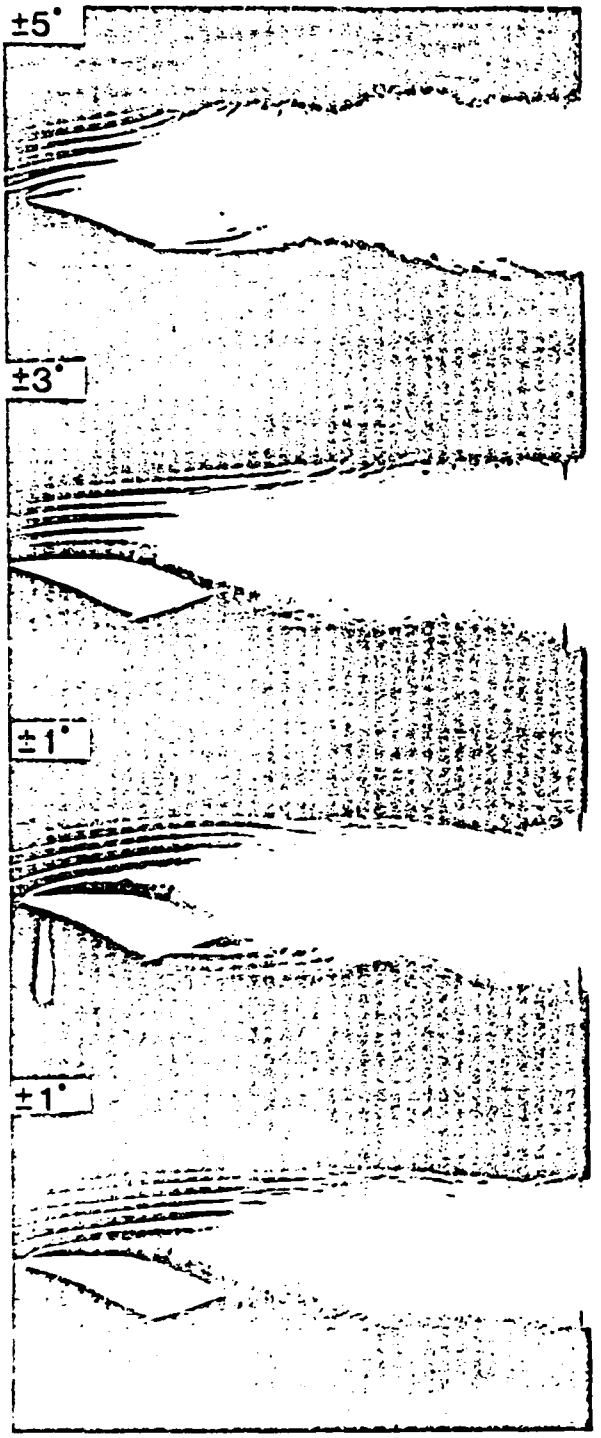

Fig. 14. Effects on the leading and trailing edge vortical interaction from variations in the oscillation angle at Re = 60,000; α_m = 15°; K = 0.5. At ±5°, the induced vortical interaction displays well-defined synchrony with airfoil oscillation. At reduced oscillation angles (±3° to ±1°), the elicited flow structure becomes less dependent on airfoil oscillation.

As expected, Reynolds number effects (Fig. 12) were inversely related to apparent vortical interaction strength. A strong interaction occurred at a Reynolds number of 60,000, as in previous results. Less definitive interactions occurred at higher Reynolds numbers. The inverse relationship between Reynolds number and leading edge vortical development also held for the trailing edge vortex; increased values of Reynolds number resulted in diminished interaction between the leading edge and trailing edge vortices.

The reduced frequency parameter of 0.5 was associated with the largest, most easily resolved vortices (Fig. 13). Lower K values were associated with reduced spatial-temporal dependence of flow field on the oscillation frequency. This reduced dependence resulted in small spatial or temporal instabilities recognized as "blurred" resolution in the visualizations of leading and trailing edge vortical interactions (Fig. 13).

The oscillation angle had a major effect on the repeatability of the flow perturbations. At higher oscillation angles (±5°) the vortical interaction was well defined both spatially and temporally, and was synchronous with airfoil oscillation. At ±3° this dependence was not as evident. Finally, at oscillation angles of ±1°, little temporal or spatial dependence on airfoil oscillation was noted for trailing edge vortex development. Without the existence of single instantaneous flow visualizations (Fig. 14), these multiple-exposure photographs would easily be mistaken as evidence for fully turbulent flow separation; the presence of vortical structures, though somewhat variable spatially and temporally, would not be recognized.

Discussion

With flow visualization and hotwire anemometry, we have documented that an airfoil oscillating sinusoidally around or above its established static stall angle elicits a leading edge vortex which then induces a trailing edge vortex. Whereas the leading edge vortex maintains flow attachment as it moves over the airfoil surface toward the trailing edge, the induced trailing edge vortex generates cataclysmic, instantaneous, complete flow separation. Visualization and anemometry findings indicated a flow perturbation continuum that extends from static stall and minimal oscillation conditions through moderate and strong oscillation conditions. Virtually the same patterns of vorticity and separation were observed across all conditions, but these patterns were temporally and spatially fixed with an oscillating airfoil, and more capricious with static stall conditions. In the latter instance, the flow perturbations gave the appearance of turbulent flow separation. The established significance of the leading and trailing edge vortices, and the empirically demonstrated control that can be exerted over the interaction of these vortices, suggest that select parameters as well as select pitching motions may yield valuable, exploitable flow attachment in the absence of cataclysmic flow separation.

The generation of the leading edge vortex and the subsequent induction of a vortex at the trailing edge were most clearly demonstrated with a large (15°) angle of attack and a large (±5°) pitching motion of the airfoil around that angle. The leading edge vortex appears as a small separation bubble as the airfoil pitches upward, accelerating the flow. The vortex becomes more discernible as the leading edge accelerates toward maximum

oscillation angles. When the airfoil begins to decelerate at maximum angles of attack, the vortex grows both away from the top airfoil surface and toward the trailing edge of the airfoil. Flow attachment is readily discernible at this time. If sufficiently energetic, the growing vortex may slow significantly in movement toward the trailing edge. At the exact moment that the first vortical streamlines of the leading edge vortex are positioned above the trailing edge, a vortex is initiated from the streamlines of the bottom surface flow. This trailing edge vortex, driven by the leading edge vortex, causes rapid, complete flow separation over the airfoil surface. The trailing edge vortex grows rapidly, with flow of opposite circulation to that of the leading edge vortex. When leading and trailing edge vortices appear to be of equal size, they shed into the airfoil wake. Interactions of these vortices in the wake lead to an apparent vertical flow, passing at freestream velocity, bounded downstream by residual leading edge vorticity and upstream by residual trailing edge vorticity. This interactive wake structure remains sufficiently cohesive to be observed many chord diameters downstream.

The major initiating determinant for the development of leading edge vortices appears to be the net acceleration about the airfoil surface. This net acceleration is composed of both a "static" acceleration component, derived from the mean angle of attack, as well as a "dynamic" component induced by rapid, large positive-angle pitching of the airfoil. Leading edge vortical development required sufficient mean angles (12.9° to 15°) under both static and oscillatory conditions. Though the magnitude of the net acceleration appears to be the most important parameter for vortical development, data were insufficient to define the exact contribution of the static and dynamic acceleration components. Qualitative consequences of each for overall vortical development were evident in both the flow visualization and hotwire data.

The vortical initiation, development, and interactions dependent on net acceleration displayed quasi-steady, temporally synchronous flow characteristics when referenced to oscillation cycle. Airfoil oscillation phase clearly provided the crucial dynamic acceleration component underlying this synchrony. Without a strong dynamic acceleration component, nonsynchronous unsteady vortical development dominated the flow. At minimal oscillation angles (±1° to ±3°), both vortical development and travel were temporally and spatially determined by airfoil oscillation phase. As both the oscillation angle and reduced frequency parameter were increased, the ensuing vortical dynamics became even more predictable. The dominant factor again was the dynamic acceleration component induced by the pitching of the airfoil. The quasi-steady vortical generation must be referenced to the airfoil oscillation; without this synchronous reference to the airfoil oscillation, the same vortical generation would appear capricious, and could be mistaken for unsteady turbulent flow separation when averaged over several oscillations.

With the airfoil at both small mean angles and small oscillation angles, much less synchronous vortical development dominated the flow structure. In these instances, the static acceleration component, with the common inherent instabilities, appeared to prevail. The leading edge and ensuing trailing edge vortical structures demonstrated much less dependence on airfoil oscillation phase. Here, the pattern of vortical development was truly unsteady when referenced to the airfoil oscillation. The quasi-steady vortical characteristics were absent. This does not, however, rule out some other as yet undisclosed periodicity underlying such flow structures.

From the observations of the current study, it is clear that elaborate flow structures can be controlled in the vicinity of an oscillating airfoil. Careful selection of the dynamic oscillation parameters in conjunction with select pitching motions may yield valuable, exploitable flow attachment while minimizing the effects of flow separation. Generation of highly repeatable flow structure with even minimal airfoil oscillation was readily documented. The leading edge vortex induced complete flow attachment. Maximal flow attachment was achieved by increasing vortex residence time on the airfoil surface. Both larger reduced frequency values and oscillation angles yielded increased residence time.

Elicitation of the trailing edge vortex led rapidly to the adverse effects of complete flow separation. Airfoil pitching phase brought the airfoil trailing edge up to meet the shedding leading edge vortex; this was seen to be an important factor in the trailing edge vortex development. By employing nonsinusoidal pitching motions or by oscillating the airfoil about different chord locations, it may be possible to minimize the trailing edge vortical growth, thereby reducing the adverse separation effects. Such studies must be pursued over a wide range of experimental conditions if exploitation of the phenomenon is to be realized.

Conclusions

Many investigators are currently involved in attempts to formalize the treatment of unsteady effects generated by an oscillating airfoil or by a pulsating flow around a static airfoil.[5,6,7,9,11,15] However, the complexity of unsteady effects hinders the comprehensive characterizations needed for precise formalization; in many instances, broad assumptions must be substituted for missing experimental data. The present studies represent an attempt to more fully describe the unsteady effects generated by an airfoil oscillating in varying amounts and speeds about fixed angles of attack. The resulting flow disturbances were complex, and required the use of rapid (≃ 7 μsec), repeated (≥20) photographic exposures synchronized with the unsteadiness generators (NACA 0012 or 0015 airfoils) to reveal both quasi-static and turbulent elements of the flow. Across a variety of combined experimental parameters, most of the resulting flow disturbances were found to be predictably synchronized, both temporally and spatially, with airfoil oscillation phase. These flow disturbances were carefully documented by visualization and hotwire anemometry.

The flow disturbances of the present study, though complex, fit along a single continuum. Static stall or dynamic stall achieved with very small dynamic parameters was typically associated with flow disturbances qualitatively quite similar to those observed with dynamic stall achieved with large dynamic parameters. The major difference was that with small parameters, flow structure exhibited wide variations in location and time when compared to any reference on the oscillating airfoil. With large dynamic parameters, both the location

and the time of flow disturbances were quite predictable and reproducible when referenced to airfoil motion. In a sense, the static and small dynamic situations elicit the most unsteady (or the least predictable) flows. In contrast, strong dynamic conditions elicit flow-airfoil interactions that are predictable enough to invite further manipulation for purposes of practical exploitation.

Two strong flow disturbances documented in the present study have received very little attention in the work of previous investigators.[4,5] It is clear that a major unsteady flow influence derives from the trailing edge vortex. We have shown that this vortex is directly proportional in size and strength to the leading edge vortex that induces it. The commonly reported cataclysmic flow separation associated with oscillating airfoils[11] most certainly is dependent upon the genesis and subsequent strength of the trailing edge vortex. The other frequently unheeded flow disturbance is the massive leading and trailing edge vortical interaction in the wake. This dramatic interaction perseveres for appreciable time and distance in the wake. Although the strength of this interaction has not been characterized, it may have serious implications for rotating blades and turbomachinery.

As noted above, these dynamically generated flow structures should be exploitable through variations in airfoil shape, airfoil motion, and, perhaps, altered boundary layers. Such dynamically generated flow structures should be analyzed through experiments on simple models. For example, current experiments[14] focus upon flow structure elicited by linear flow acceleration past a fixed airfoil. A wide range of vortical structures has been observed, and in many instances these vortices interact from leading to trailing edge of the airfoil in a manner reminiscent of the interactions observed in the present study. Similarly, the initiation and development of vortices is being studied in our laboratories using oscillating plates in a zero-flow environment. These zero-flow studies show vortical interactions similar to those observed by both Freymuth[14] and ourselves. Thus, the vorticity that we observed to be initiated by flow acceleration may exhibit some subsequent autonomy from that flow. The vortices, once formed, may be embedded in ongoing flow, but remain relatively independent of that flow. Finally, through boundary layer control experiments in our laboratories, we have discovered that most of the strong dynamically elicited flow structures are insensitive to either large pressure increments or decrements introduced at the airfoil surface near the trailing edge. Although these experiments are continuing, it is quite clear that new experimental data on unsteady phenomena can be obtained. These data should preclude much of the current need for speculation and assumptions in formal treatments of unsteady phenomena.

Acknowledgments

This work has been sponsored, in part, by the U.S. Air Force Office of Scientific Research, Grant AFOSR-81-0037, Dr. Michael S. Francis, Project Manager. The technical assistance of H. Helin, D. Sutcliffe, K. Ambrosich, L. Stodieck, C. Somps, C. Boyajian, and J. Beel is appreciated. The manuscript was prepared by L. Sweeney.

References

[1]McCroskey, W.J., "Unsteady Airfoils," Annual Review of Fluid Mechanics, 1982, pp. 285-311.

[2]Martin, J.M., Empey, R.W., McCroskey, W.J., and Caradonna, F.X., "Experimental Analysis of Dynamic Stall on an Oscillating Airfoil," Journal of the American Helicopter Society, Vol. 19, No. 1, Jan. 1973, pp. 26-32.

[3]Rossow, V.J., "Lift Enhancement by an Externally Trapped Vortex," AIAA Paper 77-672, June 1977.

[4]Ohashi, H. and Ishikawa, N., "Visualization Study of Flow Near the Trailing Edge of an Oscillating Airfoil," Bulletin of the JSME, Vol. 15, No. 85, 1972, pp. 840-847.

[5]Williams, J.C., "Flow Development in the Vicinity of the Sharp Trailing Edge on Bodies Impulsively Set into Motion," Journal of Fluid Mechanics, Vol. 115, Feb. 1982, pp. 27-37.

[6]McCroskey, W.J., "Some Current Research in Unsteady Fluid Dynamics, Freeman Scholar Lecture, 1975," Transactions of ASME Journal of Fluids Engineering, 1977, pp. 8-39.

[7]McCroskey, W.J. et al., "Dynamic Stall Experiments on Oscillating Airfoils," AIAA Paper 75-125, Jan. 1975.

[8]McAlister, K.W. and Carr, L.W., "Water Tunnel Visualizations of Dynamic Stall," Journal of Fluids Engineering, Vol. 101, Sept. 1978, pp. 376-380.

[9]Johnson, W. and Ham, N.D., "On the Mechanism of Dynamic Stall," Journal of the American Helicopter Society, Vol. 17, No. 10, Oct. 1972, pp. 36-45.

[10]Francis, M.S., Kennedy, D.A., and Butler, G.A., "Technique for the Measurement of Spatial Vorticity Distributions," Review of Scientific Instruments, Vol. 49, No. 5, May 1978, pp. 617-623.

[11]Carr, L.W., McAlister, K.W., and McCroskey, W.J., "Analysis of the Development of Dynamic Stall Based on Oscillating Airfoil Experiments," NASA TN D-8382, Jan. 1977.

[12]Helin, H.E., "Flow Visualization of Energized Separated Flow Induced by an Oscillating Airfoil," paper presented at the AIAA Region V Student Conference, St. Louis, Missouri, April 26, 1982.

[13]Robinson, M.C., Luttges, M.W., and Kennedy, D.A., "Discrete Audible Tone Generation from an NACA 0012 Airfoil," in preparation.

[14]Freymuth, P., personal communication, 1982.

[15]McCroskey, W.J. and Philippe, J.J., "Unsteady Viscous Flow on Oscillating Airfoils," AIAA Journal, Vol. 13, No. 1, Jan. 1975, pp. 71-79.